ISSN 1330-3651 (Print), ISSN 1848-6339 (Online)
UDC/UDK 621.873.034:531.35]:519.87

DYNAMICS OF THE MATHEMATICAL PENDULUM SUSPENDED FROM A MOVING MASS

Boris Jerman, Anton Hribar

Original scientific paper
The swinging of the payload is one of the most important contributors to the dynamic loading of cranes. Faster transport of the payload brings up increased swinging, larger dynamic forces, and bigger control issues. That is the reason which makes the investigation of this phenomenon an increasingly actual theme. In the paper, the horizontal inertial forces imparted by the load in the case of the linear motion of the pivot are studied by means of an appropriate mathematical model. The diagram of the factor of the horizontal inertial forces of a swinging payload mass for different conditions of operation is determined. The developed curves are compared with standard curves. It is found out that in some of the cases the standard curves are not conservative.

Keywords: *breaking phase, cranes, horizontal inertial forces, load sway, pendulum dynamics*

Dinamika matematičkog njihala koje visi na pomičnoj masi

Izvorni znanstveni članak
Njihanje tereta uveliko doprinosi dinamičkom opterećenju dizalica. Brži prijenos tereta dovodi do pojaćanog njihanja, većih dinamičkih sila i problema s upravljanjem. Zbog toga je ispitivanje ove pojave postalo vrlo aktualno. U ovom se radu horizontalne inercijske sile koje stvara teret kod linearnog gibanja okretne točke proučavaju pomoću odgovarajućeg matematičkog modela. Određen je dijagram koeficijenta horizontalnih inercijskih sila mase visećeg tereta pri različitim radnim uvjetima. Razvijene krivulje se uspoređuju sa standardnim krivuljama. Ustanovljeno je da u nekim slučajevima standardne krivulje nisu konzervativne.

Ključne riječi: *dinamika okretne točke, dizalice, horizontalne sile inercije, njihanje tereta, prijelomna faza*

1 Introduction

In general, cranes are large and heavy structures movable in different ways. Optimization of their structure is basically oriented toward savings due to smaller material and energy consumption during the production process. Smaller final weight of an overall structure also brings up smaller energy consumption during a crane's operations throughout its lifetime. All this implies smaller costs and better sustainability of the transport machine. Besides other optimization procedures the fatigue optimization of the structure is very important. For this reason the dynamic loading must be predicted in advance. Dynamic loading has different causes such as the crane's (or trolley's) accelerations and decelerations and payload swaying. Time depending loads can also be imparted by the crane's skewing [1], crane's travelling on uneven surfaces, by centripetal accelerations, etc. The earthquake excitation can in the case of more rigid structures cause large dynamic loading too [2], but it should be considered only for the cranes in nuclear facilities.

The swinging of the payload is one of the most important contributors of the dynamic loading of cranes. Faster transport of the payload brings up increased angles of declination of the suspended payload, larger dynamic forces, and more challenging control issues. That is the reason which makes the investigation of this phenomenon, which is probably one of the oldest scientific topics [4], an increasingly actual theme. So far, in the majority of published papers from this field the control strategies for load-swing suppression were studied. More of them are dealing with linear motion [4 ÷ 14] then with the curved motion [4, 15 ÷ 17] of a pivot. The payload swinging and its influence on the loading of a crane's steel structure have not been investigated to the same extent [18 ÷ 23] although these data are indispensable for optimization of the structure regarding fatigue and also for determining of maximal loading. The importance of this loading is recognized by the European standard for cranes [24], where the detailed procedure for determination of the payload inertial forces is introduced. The deceleration of the motion of the moving mass by application of the constant breaking force is its basic assumption. With the development of the electric motors, control technics, and breaking technics different acceleration and deceleration profiles of the moving mass with the pendulum (crab or crane with suspended payload) are possible. The question is challenged in the paper whether the standard procedure offers conservative solution for these deceleration types too.

In the following paragraph the horizontal inertial forces imparted on the suspended payload are briefly introduced as they are treated in the standard [24]. Then the mathematical model of a pendulum suspended from a moving mass is introduced and its structure is explained. Further the results of extensive simulations with different crane parameters and different types of deceleration of pivot are used for determination of the diagram of factor of the horizontal inertial forces of a swinging payload mass. The developed curves are compared with the curves from the standard. Finally the findings are discussed.

2 The horizontal inertial forces acting on a payload mass

2.1 The standard consideration of the horizontal inertial forces

For covering the horizontal effects of the payload dynamics during linear motion of the pivot the factor of horizontal inertial forces ψ_{h} is introduced in the standard [24]. Its purpose is fast determination of the maximal horizontal inertial force $F_{\mathrm{C,max}}$ acting due to the load acceleration or deceleration:

$$F_{C,max} = \psi_h \cdot m_1 \cdot a_{av}. \quad (1)$$

In Eq. (1) m_1 represents the payload mass and a_{av} the average acceleration or deceleration.

For determination of the horizontal inertial effects of masses, which are rigidly connected to the moving crab or crane the equation similar to Eq. (1) is used. Instead of the factor ψ_h the constant value 2 is used, assuming that maximal acceleration cannot exceed double the value of the average acceleration. Therefore, if the factor of horizontal inertial forces of the payload receives the value of $\psi_h = 2$ the maximal expected horizontal inertial force of the suspended load is equal to the maximal expected force of the rigidly connected mass. If its value is greater or smaller than 2 the influence of the swinging payload is larger or smaller respectively.

For determination of the diagram of the factor ψ_h in the standard [24] a relatively simple mathematical model of an overhead-travelling crane is used (Fig. 1) where the entirely non-deformable crane's structure is assumed. The load carrying rope is also assumed to be non-extendible but easy to bend. The dissipative effects affecting the motion of the crane or crab and the motion of the payload are neglected. The small angles φ of the swinging of the payload are assumed. The linear motion of a load suspension point (pivot) is assumed and the breaking phase from a constant speed of the pivot to the standstill is observed. The system of two second-order differential equations is solved analytically for the case of breaking with the constant breaking force F and the results are introduced in the corresponding diagram where ψ_h is plotted against the factor β for different values of factor μ. The factor β is defined as the ratio between the acceleration time t_{acc} and the period of oscillation t_1 of the load suspended on the rope looked at as a mathematical pendulum:

$$\beta = \frac{t_{acc}}{t_1}. \quad (2)$$

The factor μ is defined as the ratio between the payload mass m_1 and the mass m, which is defined as the sum of masses of all the parts that move together with the pivot (including the inertia effects of the rotating parts of the corresponding driving mechanism and excluding the payload mass m_1):

$$\mu = \frac{m_1}{m}. \quad (3)$$

It describes the influence of the sway of the payload on the movement of the pivot. The factor μ has (e.g. for overhead travelling cranes) values from (almost) 0 to around 5. As it can be seen from the equation (3) the zero value is reached when there is (almost) no load suspended from the rope, which automatically guarantees zero influence. On the other hand the zero influence can also be assumed in the case of the system with predefined speed where the time profile of the speed of the pivot is maintained (almost) unchanged regardless of the payload sway.

For the analytically solved system of two second-order differential equations (defined in standard [24] and discussed earlier in this section) the following rules apply. For the value of $\mu \le 1$, the factor ψ_h cannot go beyond the value of 2. This value is reached only in the case when the factor β reaches or goes beyond the critical value ($\beta \ge \beta_{crit}(\mu)$). If $\beta \ge \beta_{crit}$ the value of ψ_h should stay constant and equal to 2. For the value of the $\mu > 1$ the value of ψ_h can be greater than 2 if $\beta \ge \beta_{crit}$ and can reach the maximum value, defined with the equation:

$$\psi_h = \sqrt{2 + \mu + \frac{1}{\mu}}. \quad (4)$$

With increasing value of factor β the value of ψ_h varies and reaches its maximum repetitively (see the solid curves in Fig. 8). In the diagram for determination of ψ_h in standard [24] the maximum value is kept for all $\beta \ge \beta_{crit}$ (see the dashed curves in Fig. 8).

Value of $\beta = \beta_{crit}$ is reached during deceleration phase if condition $\omega_r \cdot t_{dec} = \pi$ is satisfied [24], where t_{dec} is deceleration time and ω_r is auxiliary value defined by the equation $\omega_r^2 = \frac{g}{l}(1+\mu)$. Using these relations together with Eq. (2) the following equation for critical value $\beta_{crit} = \frac{1}{2 \cdot \sqrt{1+\mu}}$ is obtained.

2.2 The mathematical model

For the purpose of consideration of different types of breaking of the pivot the analytical approach is not adequate any more. Therefore a new mathematical model of an overhead travelling crane (Fig. 1) is developed and the system of two differential equations with two independent coordinates $q_1 = x$ and $q_2 = \varphi$ is solved numerically. In accordance with Fig. 1, x represents the horizontal position of the pivot and φ represents the deviation angle of the load carrying rope from the static equilibrium. To enable the comparison of the results the model is based on the model introduced in the standard [24] but the assumption of small angles of load sway is withdrawn. The motion of the pivot can be initiated or changed by means of the active force F acting on the movable structure. The model allows for arbitrary definition of the force F, which does not have to be constant through the acceleration or deceleration period. The motion of the pivot can also be predefined as arbitrary time-velocity profile. In this case the coordinate $x = x(t)$ of the pivot is known and is therefore no longer the independent coordinate.

The mathematical model shown in Fig. 1 consists of the point mass m of the movable structure (crab or crane), of the point mass m_1 of the payload and of the non-extendible load carrying rope of the length l.

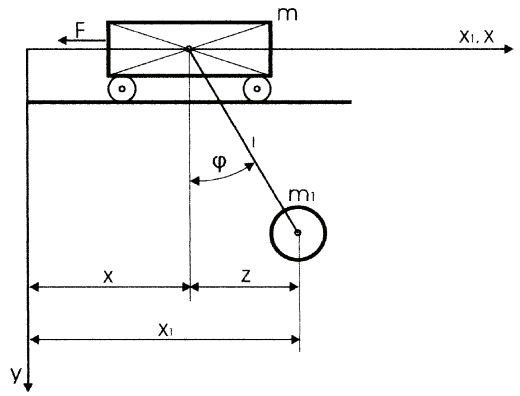

Figure 1 The basic mathematical model

Second-order Lagrange equations (Eq. 5) were used for deriving the differential equations of motion:

$$\frac{\mathrm{d}}{\mathrm{d}t}\left[\frac{\partial T}{\partial \dot{q}_j}\right] - \frac{\partial T}{\partial q_j} + \frac{\partial V}{\partial q_j} = Q_j^n \qquad j = 1, 2\,. \tag{5}$$

In Eq. (5), j represents the index of generalised independent coordinates T represents the kinetic energy of the system, V the potential energy of the system, and Q_j^n the (non-conservative) generalized forces.

The total kinetic energy T is the sum of the individual contributions of the masses m and m_1:

$$T = \frac{m \cdot \dot{x}^2}{2} + \frac{m_1 \cdot v_1{}^2}{2}, \tag{6}$$

where v_1 is the velocity of the mass m_1:

$$v_1 = \sqrt{\dot{x}^2 + l^2 \cdot \dot{\varphi}^2 + 2 \cdot l \cdot \dot{x} \cdot \dot{\varphi} \cdot \cos\varphi}\,. \tag{7}$$

The potential energy of the system is expressed as follows:

$$V = V_1 = m_1 \cdot g \cdot h\,, \tag{8}$$

where h is the height of the mass m_1 relative to its equilibrium position:

$$h = l \cdot (1 - \cos\varphi)\,. \tag{9}$$

The only non-conservative active force in the observed mathematical model is force F. Its generalised force is:

$$Q_1^n = Q_{x,F} = F\,. \tag{10}$$

Following a common procedure and taking Eq. (5) into account, the system of two second-order differential equations is derived:

$$(m + m_1) \cdot \ddot{x} + m_1 \cdot l \cdot \ddot{\varphi} = F\,, \tag{11}$$

$$m_1\ l\ \ddot{x} + m_1 \cdot l^2 \cdot \ddot{\varphi} + m_1\ l\ g\ \varphi = 0\,. \tag{12}$$

For the numerical integration of this system of equations (11) and (12) a commercial software package Mathematica was used.

The motion of the pivot generally consists of four phases: acceleration from a standstill ($\dot{x} = 0$) to desired speed ($\dot{x}$), moving with constant speed ($\dot{x}$), deceleration of the pivot back to a standstill, and observation of the pendulum motion after the pivot is brought to a standstill. Only the last two phases were of interest during the research because in the standard [24] only the breaking phase is used for determination of the ψ_h . The system of equations was solved separately for each of these two phases and the values of the parameters at the end of the preceding phase were used as the initial conditions for the next phase.

The influence of the swinging payload on the moving pivot (crab or crane) is introduced by means of the force $F_C = F_C(t)$, which is the horizontal component of the force in the load carrying rope (consisting of corresponding component of the weight of the mass m_1 and of the centripetal force imparted by the mass m_1). It is defined in Eq. (13) and shown in Fig. 2.

$$F_\mathrm{C}(t) = m_1 \cdot \left[g \cdot \cos\varphi(t) + l \cdot \dot{\varphi}(t)^2\right] \cdot \sin\varphi(t). \tag{13}$$

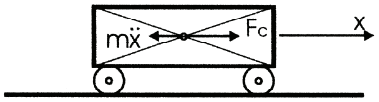

Figure 2 The position of the horizontal force $F_\mathrm{C} = F_\mathrm{C}(t)$ in the pivot

2.3 Determination of the factor of horizontal inertial forces

From the standard equation (1), the factor of horizontal inertial forces ψ_h can be defined as:

$$\psi_\mathrm{h} = \frac{F_{\mathrm{C,max}}}{F_{\mathrm{C,av}}}, \tag{14}$$

where $F_{\mathrm{C,max}}$ is the maximal horizontal force of the payload acting on the pivot and where the average horizontal force is defined as $F_{\mathrm{C,av}} = m_1 \cdot a_\mathrm{av}$.

In the research, these forces are defined for different acceleration types and other operating conditions, using the developed mathematical model (see the diagram in Fig. 7).

On the other hand these forces are in standard [24] defined as:

$$F_{\mathrm{C,av}} = F \cdot \frac{m_1}{m + m_1}, \tag{15}$$

$$F_{\mathrm{C,max}} = F_{\mathrm{C,av}} \cdot \sqrt{\left[1 - \cos(\omega_\mathrm{r} \cdot t_\mathrm{dec})\right]^2 + \frac{\omega_\mathrm{r}^2}{\omega_1^2} \cdot \sin^2(\omega_\mathrm{r} \cdot t_\mathrm{dec})}, \tag{16}$$

where the following transcendent equation is solved:

$$(\omega_\mathrm{r} \cdot t_\mathrm{dec}) + \mu \cdot \sin(\omega_\mathrm{r} \cdot t_\mathrm{dec}) - 2 \cdot \pi \cdot \beta \cdot \sqrt{1 + \mu} = 0, \tag{17}$$

to determine the product $(\omega_r \cdot t_{dec})$. When the condition $(\omega_r \cdot t_{dec}) \geq \pi$ is satisfied, the maximal horizontal force $F_{C,\max}$ appears during the deceleration and when it is not, the maximal horizontal force $F_{C,\max}$ appears after the deceleration, when the pivot is in the standstill.

2.4 Determination of the factor of horizontal inertial forces

First of all the case of breaking with the constant force ($F = F_m = \text{const}$) which is presumed in the standard was considered (Fig. 3). This case represents the real world breaking with breaks, producing constant breaking moment. This case was used for verification of the proposed mathematical model and its numerical solution.

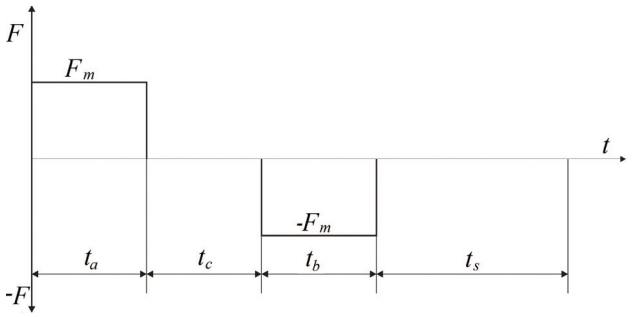

Figure 3 Acceleration and breaking with constant driving force, denoted as "*F*=const"

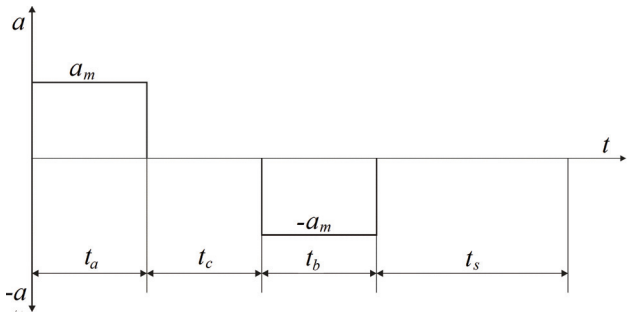

Figure 4 Acceleration and breaking with constant acceleration, denoted as "*a*=const"

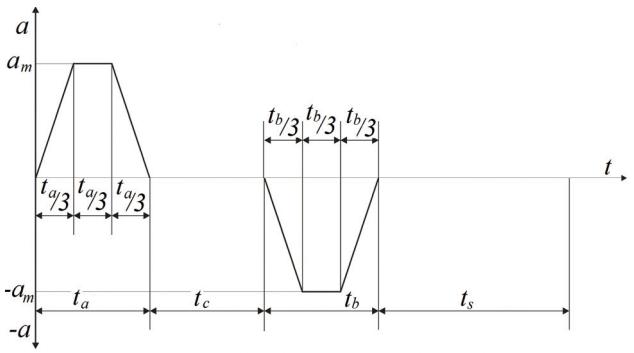

Figure 5 Acceleration and breaking with linearly variable acceleration, denoted as "*a*=linear"

Beside that also the following cases were considered which all have their real world application. The case with constant acceleration and deceleration ($a = \text{const}$) of the load suspension point during acceleration/deceleration phase (Fig. 4), the case with the linearly increasing/decreasing acceleration and deceleration (Fig. 5), and the case with the linearly increasing/decreasing driving/breaking force (Fig. 6).

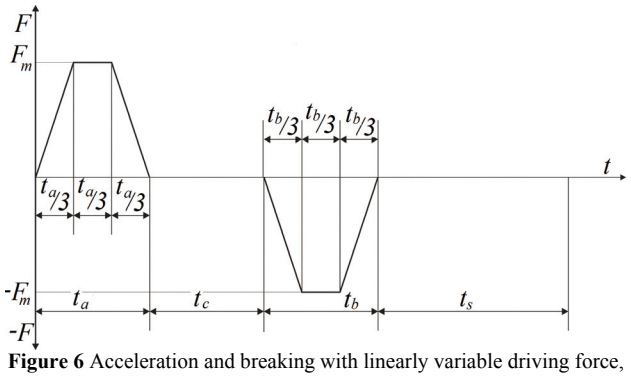

Figure 6 Acceleration and breaking with linearly variable driving force, denoted as "*F*=linear"

2.5 Diagrams of the factor of horizontal inertial forces

Using simulation results for different acceleration types (defined in 2.4) and different operating conditions the curves of the factor of horizontal inertial forces ψ_h were calculated using Eq. (14). They are introduced in Figs. 7, 8 and 9.

In Fig. 7 the curves of different types of breaking are shown, all for $\mu = 0$ to enable the comparison. The curve for "*F*=const" is close to the solution from the standard [24] as will be discussed later. It is obvious that the course of the curve for the acceleration scheme with constant acceleration (*a* = const) is more favourable than the standard one whereas the cases with linearly changeable acceleration and force (*a*=linear, *F*=linear) give higher values for ψ_h than they can be predicted from the standard. The standard prediction is exceeded for up to 28 %.

In Fig. 8 the curves for "*F*=const" and for different ratios $\mu \neq 0$ are shown. It is clear that for this type of accelerations and decelerations the standard values are covering all the values, which were predicted by means of simulations regardless of the value of the ratio μ. Exact matching of the standard and simulated curves in the first part of the diagram as well as the matching of the calculated peeks with the standard constant values in the other part of the diagram is the basis for the verification of the mathematical model.

In Fig. 9 the curves for "*F*=linear" and for different ratios $\mu \neq 0$ are shown. It is clear that for this type of accelerations and decelerations the standard values for ψ_H can be exceeded for ratios $\mu \leq 2$, whereas for ratios $\mu \geq 3$ the standard curves are on the safe side. The standard prediction is exceeded for up to 21 %.

3 Conclusions

An investigation of the horizontal inertial forces imparted to the payload during deceleration of the linear motion of the moving mass with suspended load is conducted for different deceleration types with the intention of comparison of the results with the predictions in standard. For this reason the mathematical model of a moving mass (a crab or a crane) with the suspended load

was derived based on the model from the standard but without limitations regarding small angles of the load sway.

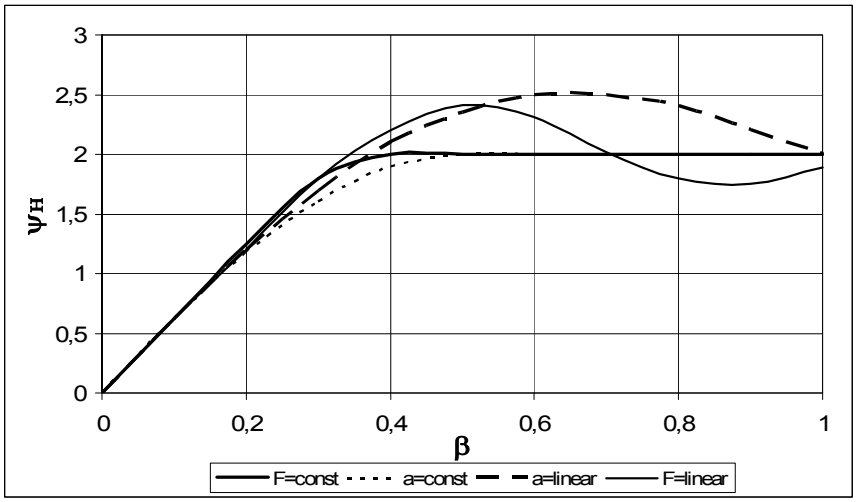

Figure 7 The curves of factor ψ_H for $\mu = 0$ and of different types of breaking

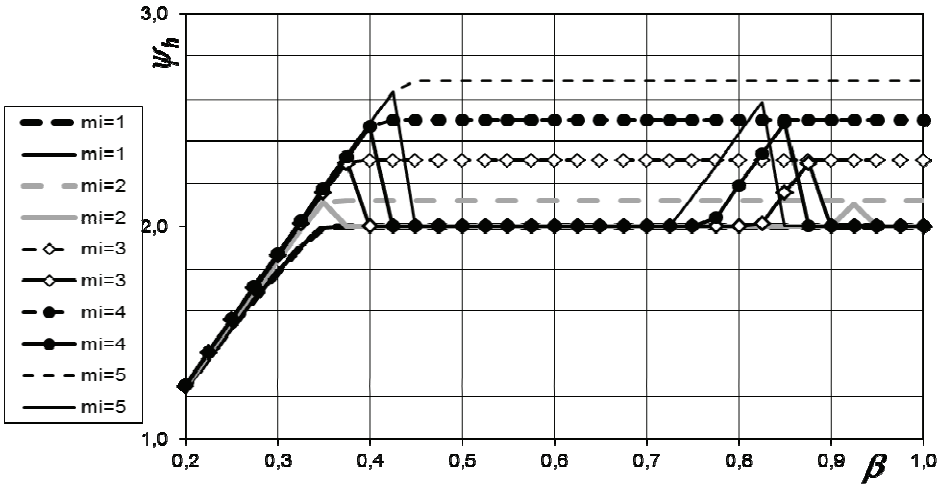

Figure 8 The curves of factor ψ_H for breaking with constant force F for different values of μ (in the legend, μ is denoted as "mi"). The calculated curves are represented with solid lines and standard curves with dashed lines.

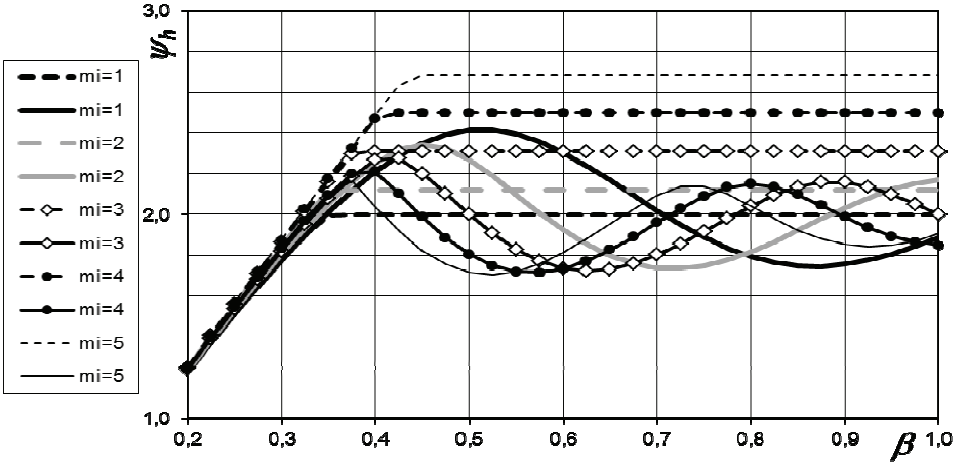

Figure 9 The curves of factor ψ_h for breaking with linearly changeable force F for different values of μ (in the legend, μ is denoted as "mi"). The calculated curves are represented with solid lines and standard curves with dashed lines.

The standard deceleration type and three additional types of breaking were considered. The results show that the course of the deceleration has strong influence on the appearing horizontal inertial force of the load. For the purpose of the verification of the derived mathematical model the breaking with the constant force was observed for ratio $\mu = 0$, and $\mu > 0$. Numerically determined curves of the factor of horizontal inertial forces ψ_h match

the standard curves. In this way the derived mathematical model was verified and used for further study. In the case of constant deceleration the values of ψ_h are equal to or smaller than the values from the standard. In other two investigated cases the factor of horizontal inertial forces ψ_H is, for some intervals of ratios β and μ, greater than the corresponding standard values. The standard prediction is exceeded for up to 28 %. This implies that the horizontal inertial loads produced by the sway of the payload can be greater than those predicted by the standard. Consequently, a more careful consideration of these loads in engineering practice is suggested.

Acknowledgment

This work has been supported by the Ministry of Education, Science, Culture and Sport of the Republic of Slovenia under the project BI-RS/12-13-050 and by the Ministry of Education and Science of the Republic of Serbia under the project 651-03-1251/2012-09/50 - The bilateral projects for scientific cooperation between the Republic of Slovenia and the Republic of Serbia in the years 2012 ÷ 2013.

5 References

[1] Mitrović, N.; Kostić, V.; Petronijević, M; Jeftenić, B. Practical Implementation of Load Sharing and Anti Skew Controllers for Wide Span Gantry Crane Drives. // Strojniški vestnik - Journal of Mechanical Engineering, 56, 3(2010), pp. 207-216.

[2] Draganić, H.; Hadzima-Nyarko, M.; Morić, D. Comparison of RC frames periods with the empiric expressions given in Eurocode 8 (Subject reviews). // Tehnički vjesnik - Technical Gazette, 17, 1(2010), pp. 93-100.

[3] Brzeski, P.; Perlikowski, P.; Yanchuk, S.; Kapitaniak, T. The dynamics of the pendulum suspended on the forced Duffing oscillator. // arXiv:1202.5937v1. Cornell University Library.

[4] Abdel-Rahman, E. M.; Nayfeh, A. H.; Masoud, Z. N. Dynamics and Control of Cranes: A Review. // Journal of Vibration and Control, 9, (2003), pp. 863-908.

[5] Lee, H. A new design approach for the anti-swing trajectory control of overhead cranes with high-speed hoisting. // International Journal of Control, 77, 10(2004), pp. 931-940.

[6] Oguamanam, D. C. D.; Hansen, J. S. Dynamics of a three-dimensional overhead crane system. // Journal of Sound and Vibration, 242, 3(2001), pp. 411-426.

[7] Bartolini, G.; Pisano A.; Usai, E. Second-order sliding-mode control of container cranes. // Automatica, 38, (2002), pp. 1783-1790.

[8] Yavin, Y.; Kemp, P. D. The application of extended inverse dynamics control. // Computers and Mathematics with Applications, 40, (2000), pp. 669-677.

[9] Zrnić, N.; Hoffmann, K.; Bošnjak, S. Modelling Of Dynamic Interaction between Structure and Trolley for Mega Container Cranes. // Math. and Computer Modelling of Dynamical Systems, 15, 3(2009), 295-311.

[10] Zrnić, N.; Bošnjak, S.; Hoffmann, K. Parameter sensitivity analysis of non-dimensional models of quayside container cranes. // Mathematical and Computer Modelling of Dynamical Systems, 16, 2(2010), 145-160.

[11] Zrnić, N.; Gašić, V.; Obradović, A.; Bošnjak, S. Appropriate modeling of dynamic behavior of quayside container cranes boom under a moving trolley. // Springer Proceedings in Physics 139, Vibration problems ICOVP 2011, pp. 81-86, 2011, Springer.

[12] Gašić, V.; Zrnić, N.; Obradović, A.; Bošnjak, S. Consideration of Moving Oscillator Problem in Dynamic Responses of Bridge Cranes. // FME Transactions, 39, 1(2011), pp. 17-24.

[13] Vladić, J.; Đokić, R.; Kljajin, M.; Karakašić, M. Modelling and simulations of elevator dynamic behaviour (Preliminary notes). // Tehnički vjesnik - Technical Gazette, 18, 3(2011), pp. 423-434.

[14] Raubar, E.; Vrančić, D. Anti-Sway System for Ship-to-Shore Cranes. // Strojniški vestnik - Journal of Mechanical Engineering, 58, 5(2012), pp. 338-344.

[15] Glossiotis, G.; Antoniadis, I. Payload sway suppression in rotary cranes by digital filtering of the commanded inputs. // Proceedings of the Institution of Mechanical Engineers, Part K, Journal of Multi-body Dynamics, 217, 2(2003), pp. 99-109.

[16] Spathopoulos, M. P.; Fragopoulos, D. Pendulation control of an offshore crane. // International Journal of Control, 77, 7(2004), pp. 654-670.

[17] Marinović, I.; Sprečić, D.; Jerman, B. A Slewing Crane Payload Dynamics. // Tehnički vjesnik - Technical Gazette, 19, 4(2012), pp. 907-916.

[18] Gašić, V.; Zrnić, N.; Rakin, M.; Consideration of a moving mass effect on dynamic behaviour of a jib crane structure. // Tehnički vjesnik - Technical Gazette, 19, 1(2012), pp. 115-121.

[19] Ghigliazza, R.M.; Holmes, P. On the dynamics of cranes, or spherical pendula with moving supports. // Int. J. of Non-Linear Mechanics, 37, (2002), pp. 1211-1221.

[20] Jerman, B.; Podržaj, P.; Kramar, J. An Investigation of Slewing-Crane Dynamics during Slewing Motion - Development and Verification of a Mathematical Model. // Int. j. mech. sci., 46, 5(2004), pp. 729-750.

[21] Wu, J. J.; Whittaker A. R.; Cartmell, M. P. The use of finite element techniques for calculating the dynamic response of structures to moving loads. // Computers and Structures, 78, (2000), pp. 789-799.

[22] Jerman, B. An enhanced mathematical model for investigating the dynamic loading of a slewing crane. // Proc. Inst. Mech. Eng., C J. mech. eng. sci., 220, 4(2006), pp. 421-433.

[23] Jerman, B.; Kramar, J. A study of the horizontal inertial forces acting on the suspended load of slewing cranes. // Int. j. mech. sci., 50, 3(2008), pp. 490-500.

[24] F.E.M 1.001. Rules for the design of hoisting appliances. 10.1998.

Authors' addresses:

assist. prof. dr. Boris Jerman
University of Ljubljana
Faculty of Mechanical Engineering
Aškerčeva c. 6
1000 Ljubljana, Slovenia
boris.jerman@fs.uni-lj.si

Anton Hribar, BSc
Litostroj Steel Ltd
Production of Quality Steel Castings
Litostrojska cesta 44
1000 Ljubljana, Slovenia
anton.hribar@litostroj.com